

UC Irvine

UC Irvine Previously Published Works

Title

Optical frequency-domain reflectometry (OFDR) using an integrated fiber tunable filter

Permalink

<https://escholarship.org/uc/item/73s3w3p4>

Authors

Chen, Z

Zhao, Y

Chen, Z

et al.

Publication Date

1999-09-25

Copyright Information

This work is made available under the terms of a Creative Commons Attribution License, available at <https://creativecommons.org/licenses/by/4.0/>

Peer reviewed

Optical frequency-domain reflectometry (OFDR) using an integrated fiber tunable filter

Yonghua Zhao*, Zhongping Chen, Johannes F. de Boer, and J. Stuart Nelson

Beckman Laser Institute and Medical Clinic, University of California, Irvine, CA 92612

ABSTRACT

We present an all-fiber, compact device for optical frequency-domain reflectometry (OFDR). The device combines a Michelson interferometer with a fiber Fabry-Perot tunable filter for rapid wavelength scanning. The free spectral range of the filter is 32 nm and scans may be completed in less than 2.5 ms. Images of the surface geometry of the material under study can be reconstructed at scan rates up to 400 Hz with an axial resolution of 20 μm .

Keywords: Reflectometry, OCT, fiber tunable filter

1. INTRODUCTION

Optical ranging and tomographic techniques have applications in various fields ranging from engineering to medicine. These techniques can be divided into three major categories: optical time-domain reflectometry (OTDR),¹ optical coherence-domain reflectometry (OCDR) or optical coherence tomography²⁻⁷ (OCT), and optical frequency-domain reflectometry^{2,8,9} (OFDR) or spectral radar. In OTDR, distance measurements are obtained in the time domain of backreflected light. Resolution is limited by the pulsewidth of the light source and suitable for measuring long distances. Both OCT and OFDR are based on coherence gating which uses a broadband light source for tomographic imaging with very high spatial resolution. In OCT systems, a broadband light source with a short coherence length (5 to 20 μm) is used. Interferometric fringes occur only when the path lengths of the reference and sample arms match within the source coherence length. Reflecting or scattering information along the axis inside the sample can be obtained by scanning the reference arm. By contrast, OFDR uses a tunable or broadband light source combined with a spectrometer. After measuring the spectrum of the interferometer output with a fixed reference arm, axial information is acquired by a Fourier transform. The advantage of OFDR is that no mechanical scanning in the axial direction is required.

In this paper, we demonstrate the application of a fiber Fabry-Perot tunable filter for OFDR. The advantages of a Fabry-Perot tunable filter are that the device can be fiber integrated and a spectrometer or tunable laser is not required. Furthermore, the scanning speed of a fiber tunable filter is faster than mechanical tuning of the spectrometer.

2. THEORY

The principle of OFDR is based on a Michelson interferometer. The current of a photodiode received in the detection arm can be represented as:

$$I(\nu, \Delta L) = \Re(I_r + I_s + 2\sqrt{I_r I_s} \cos(4\pi\nu\Delta L / c)) \quad (1)$$

Where ν is optical frequency, ΔL is the path length difference between the reference and sample arms and c is the velocity of light. I_r and I_s are the intensities coming back from the reference and sample arms, respectively. When scanning the optical frequency, the photocurrent oscillates at a frequency (f) that is

* Correspondence: Email: yzhao@bli.uci.edu; Web: <http://www.bli.uci.edu>; Tel: 949-824-3284; Fax: 949-824-8413

proportional to $2\Delta L/c$. This frequency can be determined by a Fourier transform of the photocurrent. Subsequently the path length difference can be determined as:

$$\Delta L = \frac{1}{2} cf \frac{1}{\Delta\nu / \Delta t} \quad (2)$$

where $\Delta\nu/\Delta t$ is the scanning speed of the optical frequency. When OFDR is applied to tomographic imaging of tissue where many scattering sites exist, the interference signal is:

$$I(\nu) = S(\nu) \left| 1 + \int_0^\infty a(l) \exp(i4\pi n\nu l / c) dl \right|^2 \quad (3)$$

where $S(\nu)$ is the spectral intensity distribution of the light source, $a(l)$ is the backscattered amplitude of the tissue along axial l , and n is the tissue refractive index. Information on the scattering properties of the tissue under study can be obtained by performing a Fourier transformation.

3. EXPERIMENTAL SYSTEM

In our OFDR system (Fig. 1), a superluminescent diode (SLD) with the center wavelength at 850 nm and a bandwidth of 25 nm is used as the low-coherence source. Light from the SLD and an aiming beam (He-Ne laser, 633 nm) are coupled into a fiber-optic Michelson interferometer by a 2×1 coupler. Approximately 1 mW of SLD light is coupled into the fiber and then split into reference and target arms of the interferometer by a 2×2 (50:50) fiber coupler. Stress birefringence is used to match the polarization of reference and sample beams and to optimize fringe contrast. Light in the target arm is focused onto the sample surface by a gradient-index lens (N.A. = 0.2). Two-dimensional geometric images are formed by lateral scanning the lens probe in X-Y directions. The reference arm is terminated by a stationary retroreflector. Light backscattered from the sample recombines with the reference beam within the 2×2 fiber coupler and then passed through the fiber Fabry-Perot tunable filter. Light backscattered from the sample recombines with the reference beam within the 2×2 fiber coupler and then passed through the fiber Fabry-Perot tunable filter.

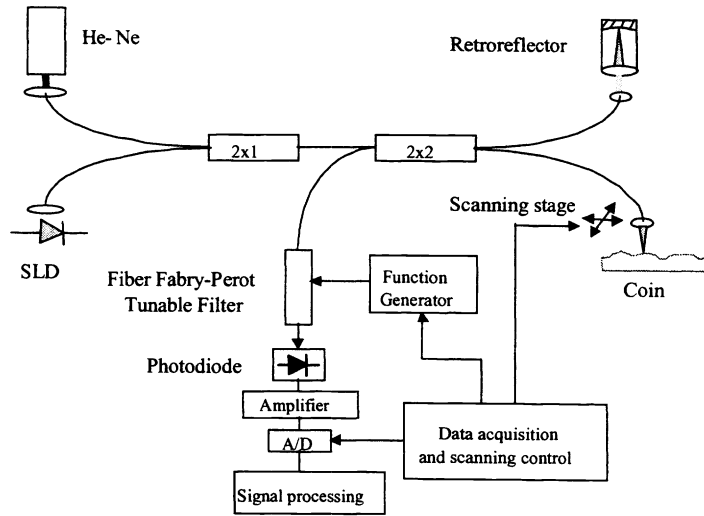


Fig.1 Schematic diagram of the experimental system. A/D, analog-digital converter.

The filter is constructed with a Fabry-Perot cavity where the distance between two cavity mirrors is controlled by a PZT. When the voltage applied to the PZT changes linearly, the wavelength of the light that can pass through the Fabry-Perot cavity also changes linearly. The transmission curve at 830 nm vs PZT voltage is shown in Fig. 2. The free spectral range of the filter is 14355 GHz (32 nm) and the finesse is 416 meaning that the axial resolution can be as high as 20 μm and the scanning range is up to 0.4 mm. The tuning voltage for the total free spectral range is only 12 V, and does not require a special amplifier. SLD's

spectrum measured by the fiber FP tunable filter driven with a 12 V saw-tooth signal is shown in Fig.3. Although the free spectral range is slightly smaller than the full bandwidth of the SLD, the distortion of spectrum is very small. As a result, the axial resolution does not decrease.

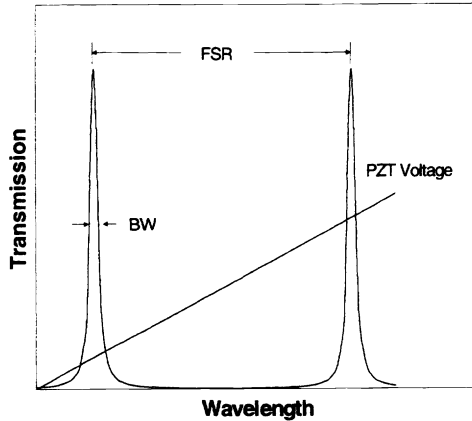


Fig. 2. Transmission curve of the fiber Fabry-Perot tunable filter when driven by a linear PZT voltage. FSR (free spectral range) is 32 nm and BW (bandwidth) is 0.077nm.

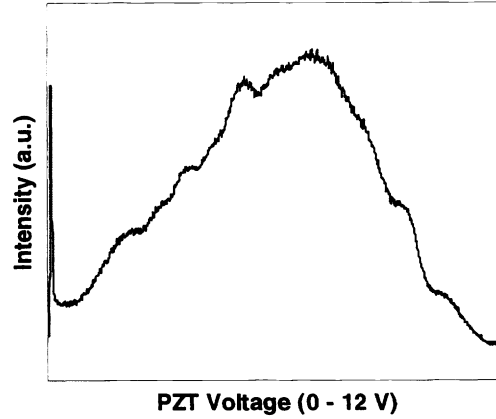


Fig. 3. Spectrum of the SLD measured by the fiber Fabry-Perot tunable filter. The spectral scanning range is equal to the free spectral range of the filter (32nm).

A silicon photovoltaic receiver located after the fiber Fabry-Perot filter measured the spectrum of the interferometer. The signal was digitized with a 16-bit analog-digital converter and then transferred to a computer workstation for processing. All devices here, including the function generator to drive the PZT, scanning stage driver, and A/D converter, were controlled and synchronized by a PC through a GPIB interface. The maximum sampling frequency of the A/D converter was 100 kHz which limits the scanning speed of the filter to 100 Hz because 1024 sample points are chosen for each spectral scanning. However, the scanning speed can be as high as 400 Hz without sacrificing resolution. The finesse of the Fabry-Perot filter will decrease if the driven frequency exceeds 500 Hz.

4. RESULTS

Figure 4 shows the digitized interferograms and the corresponding 16-bit Fourier transforms. The two scans were taken from a sample with different path lengths between the two arms of the Michelson interferometer. It can be noted that different interferometer arm mismatches are encoded as modulation frequencies of the detected interferograms, which is described above in the theory section. Since OFDR relates the absolute path difference between the different arms in the interferometer to the modulation frequency of the interferograms, it is not possible to distinguish which of the interferometer path lengths is actually longer. To avoid any misinterpretation in the acquired images it is important that the zero path length difference is set at the top surface of the sample at the beginning of the experiment.

To demonstrate the imaging capability of the system, we reconstructed an image of the surface geometry of the lettering on a U.S. dime coin. The letters of "USU NUM" are shown in Fig. 5. Although the pixel size here is approximately 50 μm , the image resolution could be as small as 10 μm and is only determined by the focusing lens. To obtain the three-dimensional image we moved the probe containing the focusing lens on the translation stages over an area of 5 mm \times 5 mm.

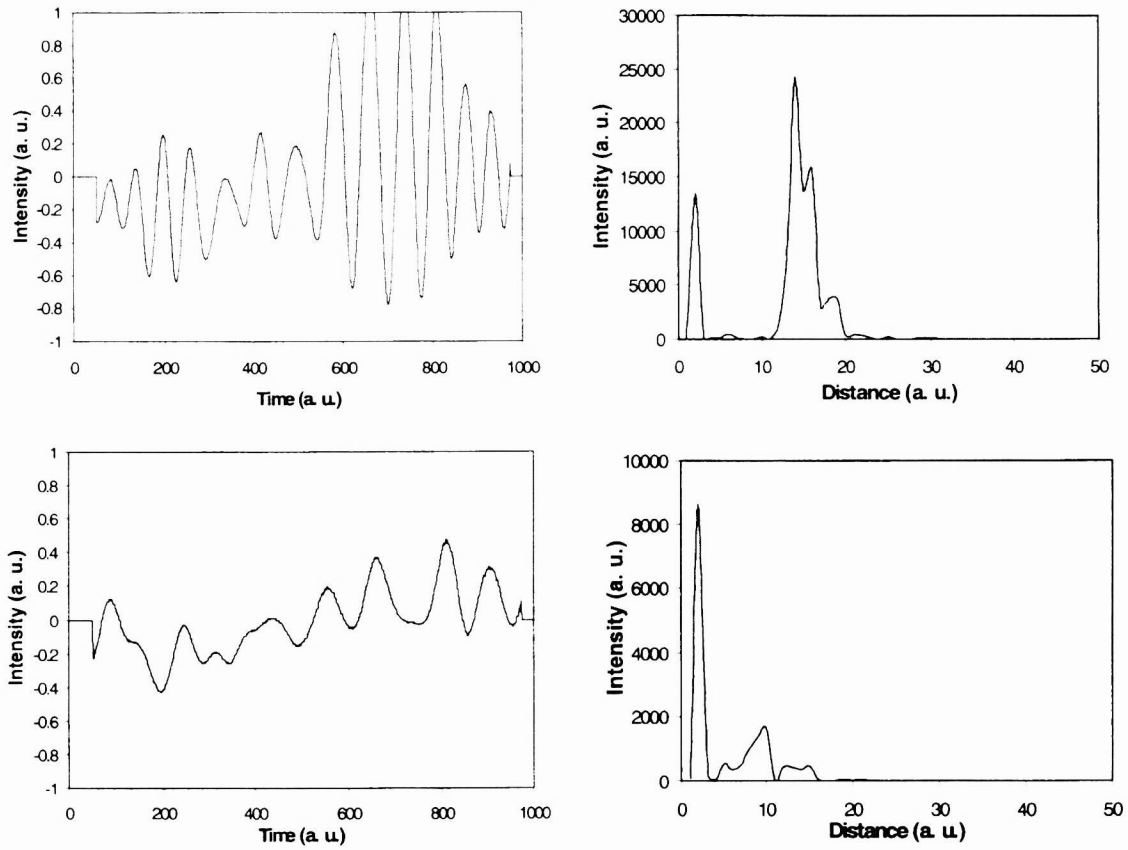


Fig.4. Fringes of the interferometer at different locations on the sample (left) and corresponding Fourier transform (right).

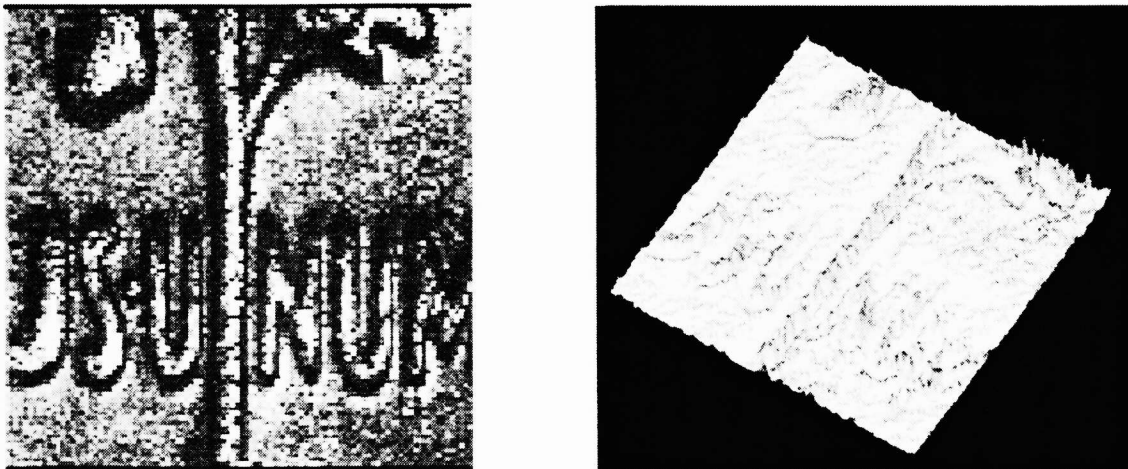


Fig. 5. Left, reconstructed surface image of a U. S. dime coin, white represents the elevated letters. Right, corresponding geometric image.

5. CONCLUSIONS

In conclusion, we have demonstrated the operation of an OFDR system using a rapid scanning, fiber-integrated filter. The filter was constructed using a Fabry-Perot cavity and PZT which can be driven at frequencies as high as 400 Hz. Using such a compact system, the geometric image of a sample surface can easily be reconstructed with a depth resolution of 20 μm . The potential extension of this technique using a high power light source and new fiber filter with a broader spectral scanning range is higher resolution and higher dynamic range for OCT imaging.

ACKNOWLEDGMENTS

We thank Shyam Srinivas and Christopher Saxer for helpful discussions and comments. This work was supported by research grants awarded from the Whitaker Foundation (WF-23281) and the Institute of Arthritis and Musculoskeletal and Skin Diseases at the National Institutes of Health (AR43419). Institutional support from the Office of Naval Research (N00014-94-1-0874), Department of Energy (DE-FG03-91ER61227), National Institutes of Health (RR-01192), and the Beckman Laser Institute and Medical Clinic Endowment is also gratefully acknowledged.

REFERENCES

1. S. D. Personick, "Photon probe-an optical-fiber time-domain reflectometer," *Bell Syst. Tech. J.*, **56**, pp. 355-366, 1977.
2. D. Uttam and B. Culshaw, "Precision time domain reflectometry in optical fiber systems using a frequency modulated continuous wave ranging technique," *J. Lightwave Technol.*, **LT-3**, pp. 971-977, 1985.
3. R. C. Youngquist, S. Carr, and D. E. N. Davies, "Optical coherence-domain reflectometry: a new optical evaluation technique," *Opt. Lett.*, **12**, pp. 158-160, 1987.
4. K. Takada, I. Yokohama, K. Chida, and J. Noda, "New measurement system for fault location in optical waveguide devices based on an interferometric technique," *Appl. Opt.*, **26**, pp. 1603-1606, 1987.
5. H. H. Gilgen, R. P. Novak, R. P. Salathe, W. Hodel, and P. Beaud, "Submillimeter optical reflectometry," *J. Lightwave Technol.*, **7**, pp. 1225-1233, 1989.
6. Z. Chen, T. E. Milner, D. Dave, J. S. Nelson, "Optical Doppler tomographic image of fluid flow velocity in highly scattering media," *Opt. Lett.*, **22**, pp. 64-66, 1997.
7. Z. Chen, T. E. Milner, S. Srinivas, A. Malekafzali, X. Wang, M. J. C. Van Gemert, J. S. Nelson, "Imaging in vivo blood flow velocity using optical Doppler tomography," *Opt. Lett.*, **22**, pp. 1119-121, 1997.
8. B. Golubovic, B. E. Bouma, G. J. Tearney, and J. G. Fujimoto, "Optical frequency-domain reflectometry using rapid wavelength tuning of a Cr^{4+} :forsterite laser," *Opt. Lett.*, **22**, pp. 1704-1706, 1997.
9. G. Hausler and M. W. Lindner, "Coherence radar and spectral radar: New tools for dermatological diagnosis", *J. Biomedical Opt.*, **3**, pp. 21-31, 1998.